Research Article | Vol. 27, No. 11 | 27 May 2019 | OPTICS EXPRESS 15575
Optics EXPRESS

Implementation and characterization of a thermal infrared laser heterodyne radiometer based on a wavelength modulated local oscillator laser

PEDRO MARTÍN-MATEOS,[1,*] ANDREAS GENNER,[2] HARALD MOSER,[2] AND BERNHARD LENDL[2]

[1]*Electronics Technology Department, Universidad Carlos III de Madrid, C/Butarque 15, 28911 Leganés, Madrid, Spain*
[2]*Institute of Chemical Technologies and Analytics, Technische Universität Wien, Getreidemarkt 9/164-UPA, 1060 Vienna, Austria*
[*]*pmmateos@ing.uc3m.es*

Abstract: This article presents the first implementation and the experimental characterization of a thermal infrared wavelength modulation laser heterodyne radiometer (WM-LHR) based on an external cavity quantum cascade laser. This novel WM-LHR system has demonstrated calibration-free operation, a superior signal to noise ratio and, more importantly, has opened the door for cost-efficient wide spectral range laser heterodyne radiometry in the near future.

1. Introduction

Optical spectroscopy is arguably the technique with the highest potential for atmospheric sounding: the Total Carbon Column Observing Network (TCCON) [1,2], the Thermal and Near infrared Sensor onboard the Greenhouse Gases Observing Satellite (GOSAT) [3] or the Orbiting Carbon Observatory 2 spectrometers [4,5] are indeed some of the most outstanding examples of the capabilities of the approach. The sophisticated spectral analyzers mentioned above, which provide reliable estimations of the concentrations of atmospheric constituents such as water vapor, carbon dioxide, methane, and nitrous oxide, have been implemented utilizing Fourier Transform (FTS) or grating spectrometers (as virtually any other, ground-based or spaceborne, optical atmospheric sounding infrastructure nowadays). However, and strongly supported by the advent of high quality, robust and compact laser sources, many stunning instrument designs and experimental demonstrations are paving the way for Laser Heterodyne Radiometers (LHR) to become the terrestrial and planetary atmospheric optical sounding tool of the future [6–12].

LHR systems provide very high sensitivity, ultra-narrow optical resolution, very confined field-of-view, and, due to low component count, reduced cost, high reliability, and a huge potential for ruggedization and miniaturization [13,14]. The LHR method has, nevertheless, remained essentially unchanged from the very first demonstrations performed by Menzies and Shumate [15,16] in the early seventies and, up to this day, most developments have been focused on the adoption of higher-performing components. It was only very recently that a new LHR spectral interrogation procedure, Wavelength Modulation Laser Heterodyne Radiometry (WM-LHR) [17], was proposed as a noteworthy performance enhancement step. WM-LHR is based on the use of a wavelength-modulated local oscillator (LO) laser in a manner similar to the vastly used Wavelength Modulation Spectroscopy (WMS) technique [18]. A preliminary WM-LHR near-infrared system implementation [17], based on optical communication components, recently demonstrated a very promising boost in performance and consistency. This paper now presents the first implementation of a thermal infrared (TIR) WM-LHR based on an external cavity quantum cascade laser (EC-QCL) and provides a

#360754 https://doi.org/10.1364/OE.27.015575
Journal © 2019 Received 21 Feb 2019; revised 28 Apr 2019; accepted 7 May 2019; published 17 May 2019

Optics EXPRESS

thorough characterization of the system and a comprehensive comparison of performance with the traditional LHR method. This novel WM-LHR system has demonstrated calibration-free operation, a superior signal to noise ratio and, more importantly, has opened the door for wide spectral range radiometric measurements in the near future. The results yield a very clear and conclusive representation of the new and unique capabilities of this novel spectral analysis approach.

2. Wavelength modulation laser heterodyne radiometry

2.1 Fundamentals of the method

The block diagram of the WM-LHR architecture can be seen in Fig. 1. The incoming optical signal is combined with the LO on a beam splitter and focused into the detector. The RF chain maintains a classical design based on amplification, band-pass filtering, RF power detection and lock-in signal demodulation. A ramp modulation signal is applied to the laser for frequency sweeping in order to facilitate the spectral interrogation of the incoming signal. Contrary to traditional LHR [19], WM-LHR adds a sinusoidal frequency modulation to the ramp signal of the laser that completely redefines the functioning of the heterodyne radiometer. In this way, the traditional spectral intensity detection performed by LHR is now converted into optical intensity differentiation (the presence of an absorption line gives rise to harmonics of the modulation signal that can be utilized to infer the composition of the gas sample under analysis) providing several noteworthy advantages in the process.

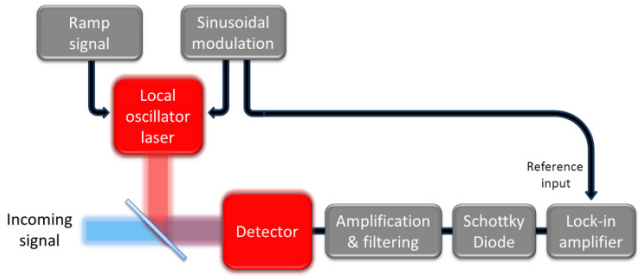

Fig. 1. Schematic of a WM-LHR system.

2.2 Thermal infrared wavelength modulation laser heterodyne radiometry with an external cavity quantum cascade laser

A photograph of the experimental TIR WM-LHR implementation based on an EC-QCL is shown in Fig. 2. A continuous wave mode-hop-free EC-QCL (41078-MHF, Daylight Solutions, Inc., USA) with a wavelength tuning range from 7.64 to 8.22 μm (1319 to 1217 cm^{-1}) and a maximum power output of 225 mW is employed. The laser frequency is slowly swept across the spectrum of interest using a ramp signal generator connected to the piezo element that controls the external cavity length. A much faster sinusoidal modulation of the laser is achieved by the direct modulation of the QCL current through the internal bias Tee circuit.

The first optical component of the set-up is an uncoated 4 mm thick calcium fluoride window acting as a beam splitter that sends roughly the 95% of the power emitted by the laser to a beam block. The remaining light is redirected to the next stages of the heterodyne radiometer (a second beam-stopper eliminates the reflection on the backside of the beam-splitter). This approach is preferred over the traditional laser intensity control based on polarizers, as it provides an improved performance with respect to interference fringes. Subsequently, beam expansion, required for an adequate spatial overlapping with the optical signal, is realized by means of two 90 degrees gold-coated off-axis parabolic mirrors with focal lengths of 1 and 6 inches. The total diameter of the laser beam is, in this manner, expanded up to 12 mm. A second calcium fluoride window combines the LO light with the

Optics EXPRESS

signal (5:95) and redirects the resulting beam to a parabolic mirror that focus the light into the thermal detector. A thermoelectrically cooled photovoltaic detector (PVI-4TE-10.6-1x1, Vigo Systems S. A., Poland) with a high speed (450 MHz) transimpedance preamplifier has been employed in the experimental demonstrations presented in this paper. The use of a thermoelectrically cooled detector instead of the conventional liquid nitrogen unit is utterly important to facilitate the eventual field deployment of the radiometer. No modifications were made to the detector to reduce the noise level. To ensure maximum consistency in the experimental results, a regular optical signal is replicated with a 12 V silicon carbide IR source (an area of roughly 70×10^{-9} m^2 of the source is imaged into the detector) and an off-axis parabolic mirror that collimates part of the emitted radiation through a 30 mm gas cell with calcium fluoride windows. A band-pass optical filter (7.5 to 8.5 µm) finally restricts the optical bandwidth of the incoming signal before combination with the LO for spectral interrogation. Different gas concentrations were pumped into the cell for the characterization of the performance of the system. An optical chopper, which is disabled during WM operation, is also included to benchmark the performance of WM-LHR with the traditional LHR method. The RF processing chain is comprised of a low-noise 24 dB amplifier (ZFL-500LN, Mini-Circuits Inc., USA), a 50 MHz to 100 MHz band-pass filter and a Schottky detector (EZR0120A3, Eclipse Microwave Inc., U.S.A.). The dual-sideband optical resolution of the spectrometer is, therefore, 100 MHz or 0.003 cm^{-1}.

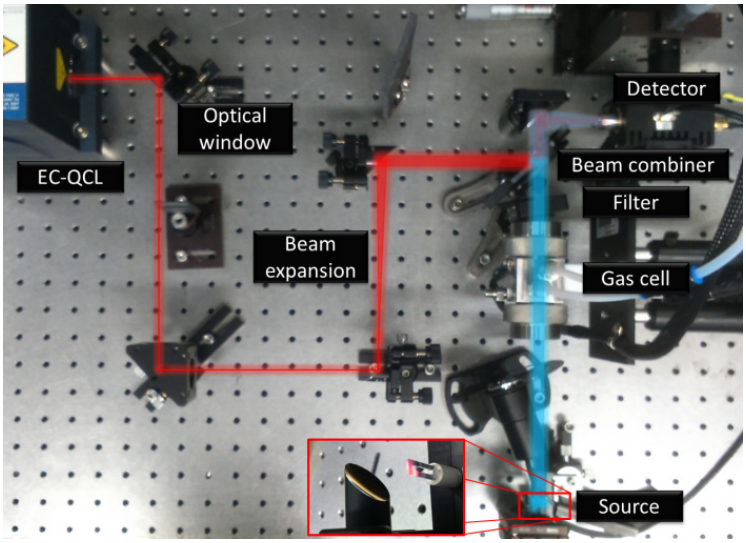

Fig. 2. Photograph of the WM-LHR implemented in the laboratory. The red and blue lines represent the optical path of the local oscillator laser and the thermal signal respectively.

The EC-QCL was tuned to 7.87 µm (1270.8 cm^{-1}) to target methane inside the cell. The laser was operated at a forward current of 375 mA to ensure a LO power reaching the detector of 150 µW; this intensity level was found to be the optimum operation point of our detector (the power passing through the cell in these conditions is approximately 5 mW). The sinusoidal modulation of the current of the EC-QCL was performed at 185 Hz and 1 Vp (for a total frequency deviation of 0.0002 pm or 0.033 cm^{-1}) in order to achieve a fast wavelength modulation of the LO with an optimum modulation index of about 2.2 times the linewidth of the molecular transition [17]. Besides this, a sawtooth signal, amplified by a piezo driver up to 20 V peak to peak, was utilized for fine spectral interrogation. The power dissipated by the infrared source and the gas concentration in the cell were widely tuned during several tests to accurately characterize the effectiveness of the WM-LHR method.

Optics EXPRESS

3. Experimental results

3.1 Experimental validation and WM-LHR calibration-free operation

The WM-LHR output signals for a CH_4 sample with a concentration of 20% in nitrogen at 60 mbar (restricted by the maximum modulation current of the laser) using a 30 mm gas cell, an electrical power of 12.5 W dissipated on the thermal infrared emitter, 330 ms of integration time in the lock-in amplifier and a total sweep time of 15 s are shown in Fig. 3. Interference fringes within the cavity of the laser employed in the set-up generate a strong residual amplitude modulation (RAM) in the first harmonic of the modulation signal. This RAM, for a measurement in which only the LO signal is allowed to reach the detector is shown in red in Fig. 3(a) (red) together with an actual measurement of the methane sample (blue). The abscissa axis was calibrated prior to the measurements using a 50.815 mm germanium etalon. The 1f WM-LHR signal can be straightforwardly baseline-compensated by a quadratic curve fitting (R^2 = 0.9995) and the resulting waveform is plotted in Fig. 3(b) (which corresponds directly to the first derivative of the spectrum of the input signal). The second (2f) and third (3f) harmonics of the modulation frequency can be seen in Figs. 3(c) and 3(d) correspondingly.

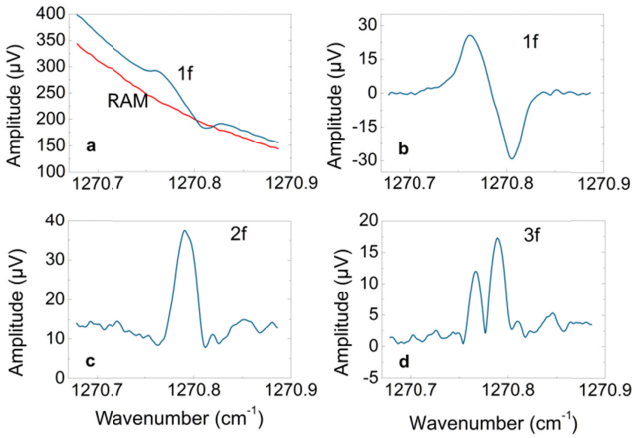

Fig. 3. WM-LHR signals: (a) RAM and 1f, (b) baseline-compensated 1f, (c) 2f and (d) 3f.

As expected from WMS, the amplitudes of the harmonics depend on both the concentration of gas in the sample and the power emitted by the thermal source, therefore a normalization procedure is required to enable calibration-free operation. Luckily, the baseline level of the 1f harmonic provides a direct measurement of the optical power at the entrance of the spectrometer that can, hence, be used to enable calibration-free WM-LHR sample characterization. The RAM of the laser source has been long used in calibration-free WMS approaches for intensity normalization [20] and a similar procedure can now also be employed for WM-LHR. As seen in Fig. 3(a), the incoming optical intensity generates an increase in the baseline level beyond the signal caused by the RAM of the laser. As a matter of fact, this increase is directly proportional to the source light intensity, and therefore the intensity of the incoming optical signal can be accurately determined. Then, the intensity-normalization of the 1f, 2f and 3f output signals will provide a set of waveforms that depend exclusively on the absorption line depth and that can hence be directly related to the gas concentration (column density).

In the experiments presented in this paper, the best calibration-free performance has been obtained by dividing the peak-to-peak 1f signal by the offset of the quadratic fitting of the baseline. For the evaluation of this calibration-free strategy, six individual measurements were taken at three methane concentrations (4%, 6% and 10%) and for electrical power levels

Optics EXPRESS

dissipated in the thermal source of 6.5, 8.5, 9.75 and 12.75 W (for a total of 72 spectral measurements). The normalized 1f amplitudes averaged for each set of six measurements are shown in Fig. 4. The experimentally obtained precision of the normalization procedure is 2.4% for an integration time of the lock-in amplifier of 330 ms and a sweep time of 15 s. This result demonstrates that WM-LHR can accurately operate in calibration-free conditions with independence of the intensity of the source and providing high consistency and fast measurement rates. In experimental scenarios in which non-absorbing spectral regions are unavailable or precluded by the limited tunability of the laser source, any other regular WMS signal normalization strategy, such as the widely used WMS-2f/1f, could be employed.

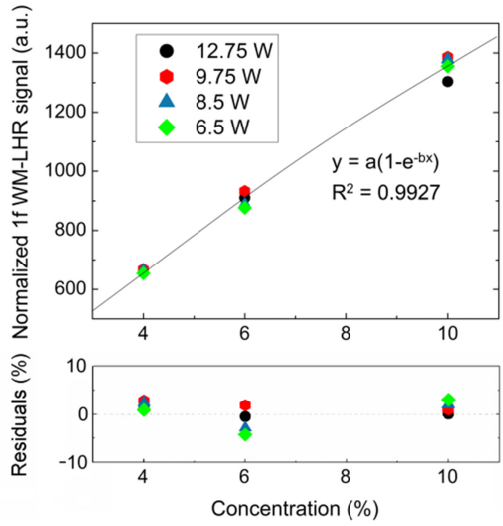

Fig. 4. Calibration-free WM-LHR performance.

4. Analysis of performance and comparison with laser heterodyne radiometry

Some of the features and advantages provided by WM-LHR can be better illustrated when the technique is benchmarked against LHR. Therefore, as presented before, an optical chopper was included in the set-up and WM-LHR and conventional LHR measurements were alternatively taken under the same operational conditions. During WM-LHR operation the chopper is stopped, the blades set out of the optical path of the signal and the LO frequency is modulated as described in the previous sections of the paper. In LHR mode, the frequency modulation of the LO source is disabled and the optical chopper is activated. The modulation and chopping frequencies were set to the same value: 185 Hz, to avoid misleading results due to the frequency response of the detectors or the RF processing chain.

4.1 Baseline and signal normalization in LHR

An LHR measurement taken in the same conditions described for Fig. 3 can be seen in Fig. 5 for a straightforward comparison. Three separate areas have been highlighted to differentiate different situations: in (1) both the signal and the laser beams are blocked, only residual noise is visible, in section (2) the LO is blocked and the incoming signal is let through to reach the photodetector, a noticeable baseline signal is generated under these circumstances, and in (3) both the signal and the LO are allowed to impinge on the detector, the overlap between the spectrum of the incoming light and the intensity response to frequency-sweeping of the laser is apparent. With a system implementation based on an off-the-shelf thermoelectrically cooled detector and a 1000 nm band-pass optical filter, an LO-independent baseline (shown in section (2) of the Fig.) appears as a consequence of the non-linearities in the gain profile of

Optics EXPRESS

the detection chain. The strong changes in DC level induced by chopping the optical signal produce the modulation of the gain of the preamplifier (the baseline is a consequence of the modulated amplification of the noise generated by the system front-end). Even though narrower optical filters would lessen the baseline level, this issue has still to be considered in order to guarantee the accuracy of the measurements. In the same way, gain non-linearities also produce the compression of the absorption line-shape by factors that depend on the intensity of the incoming signal, which complicates LHR calibration-free operation. As a matter of fact, if not compensated, the raw transmittance measurement presented in Fig. 5 induces an error by a factor of approximately 8 in the estimation of the concentration of methane in the sample due to non-linearities.

By contrast, in WM-LHR no signal chopping is required and therefore the DC operation point and the gain of the detection chain remains constant during the whole spectral acquisition (regardless of the quality of the detector) producing no spectral distortion and thus enabling a straightforward compensation. The gain non-linearity issue is often overlooked by papers on the topic, but it is a very important factor to consider when implementing a LHR system with cost-effective components. This first comparison reveals that WM-LHR puts far less strain than LHR in the performance of the components required for the implementation of the set-up.

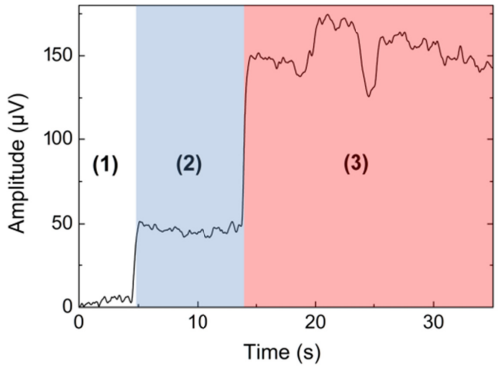

Fig. 5. LHR measurement. The different zones identify (1) signal and LO blocked, (2) signal reaching the detector and LO block and (3) both signal and LO in the detector.

4.2 Signal to noise ratio

The characterization of the SNR provided by the two techniques was carried out through a data set in which ten consecutive spectra are digitized for both methods for different integration times of the lock-in amplifier. A gas concentration of 20% and 12 W of electrical power in the thermal source were employed. The SNR of the WM-LHR harmonics is determined as the peak to peak signal divided by the standard deviation of the baseline far from the molecular resonance (in a nearby region not affected by the spectral line) calculated for a wavelength range equal to three times the linewidth of the transition covering several background fringes. In the case of LHR, the SNR is obtained as the ratio between the depth of the absorption line and, as before, the standard deviation of the baseline out of the molecular transition.

Optics EXPRESS

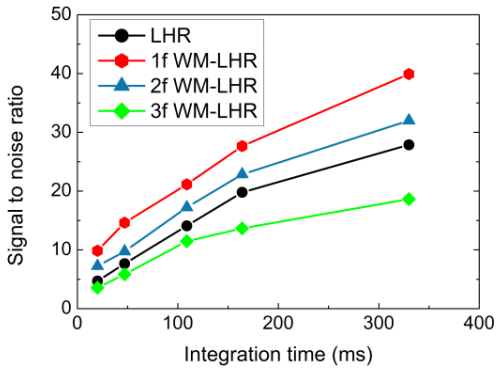

Fig. 6. Signal to noise ratio with respect to the integration time of the lock-in amplifier.

As shown in Fig. 6, the SNR of the thermal infrared radiometer provided by 1f and 2f WM-LHR noticeably exceeds that of the conventional LHR method. This is expected, as in WM-LHR the modulation is performed directly by an electronic reference signal, while a mechanical system with far greater phase jitter and frequency drifts is utilized by LHR. Interference fringes in the cavity of the particular laser employed are the main SNR restricting factor in the implemented WM-LHR system. The differences in SNR could be even more apparent when laser diodes (with much lower RAM) are employed in systems in which a great level of amplification is required [17].

4.3 Out-of-band signal rejection

Even though the use of LHR has routinely been restricted to very narrow (single absorption line) spectral ranges, the surge of robust widely tunable laser technology promises to permit the development of a new generation of wide span heterodyne radiometers. In the traditional LHR approximation highly selective optical filters are employed to narrow down the spectral span of the signal to be analyzed because of the reasons presented in Section 4.1. Set-ups with a wide spectral coverage require a method with a superior out-of-band intensity rejection such as WM-LHR. In this section, the ability of the traditional and the WM-LHR approaches to operate without optical filters are analyzed. A series of measurements were carried out in which the optical filter that restricts the wavelength range of the incoming signal is placed in the system and subsequently removed. A gas sample with 10% methane diluted in nitrogen at 60 mbar was pumped into the cell, the integration time of the lock in amplifier was adjusted to 100 ms and the period of the ramp signal to 20 s. A traditional LHR measurement in which four line sweeps are performed, two with optical filter and two without the optical filter, is shown in Fig. 7(a). Even though the optical power density of the signal in the spectral range interrogated by the laser rises only by roughly 40% (due to the absence of the optical losses of the filter), the baseline is increased by more than an order of magnitude due to optical power reaching the detector at wavelengths that are far from the region of interest. As previously presented, the pronounced step changes in the intensity of the incoming power (that result from the need of chopping the input signal) generate a substantial gain modulation due to the non-linearities of regular detectors and amplifiers. This issue is strongly noticed if out-of-band radiation is allowed into the detector, as is this case. On the contrary, both the baseline and the WM-LHR signal, shown in Fig. 7(b), are incremented by a factor that is equal to the inverse of the transmittance of the optical filter, not being influenced by out-of-band optical radiation. The reason being that, whereas signal chopping in LHR generates high amplitude optical pulses, in WM-LHR the only intensity fluctuations are those from the RAM of the laser that are miniscule compared to the DC intensity level. Therefore, WM-LHR measurements are consistently taken at a constant gain value (and with no distortion of the

line shape due to the gain saturation profile) allowing for a far greater dynamic range. This behavior becomes even clearer in Figs. 7(c) and 7(d), in which the baseline-compensated LHR and WM-LHR signals measured with and without the optical filter are represented. Whereas LHR is unable to operate without the filter, WM-LHR performs without issues, even providing an improved SNR due to the higher amplitude of the 1f signal (shot-noise in the system is not the main noise contributor).

Summarizing, the increased dynamic range and the possibility to operate without optical filters provided by WM-LHR enable the implementation of highly flexible wide coverage radiometers that allow taking full advantage of the characteristics of modern widely tunable laser sources.

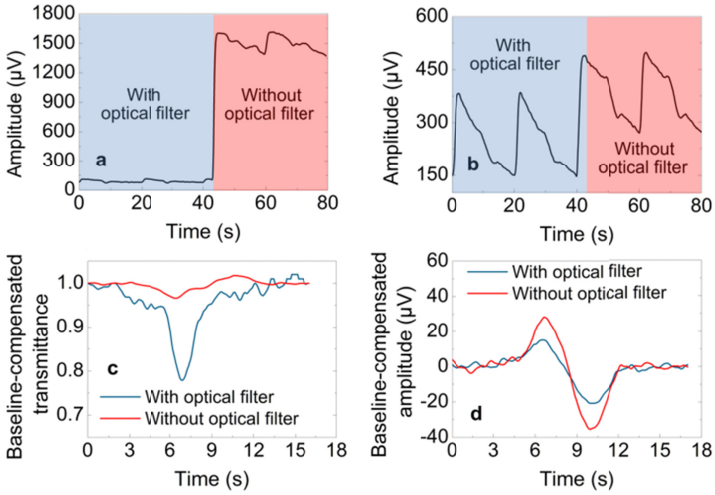

Fig. 7. Behavior of LHR and WM-LHR with and without optical filter: raw (a) LHR and (b) WM-LHR measurements; baseline-compensated (c) LHR and (d) WM-LHR signals.

5. Conclusion

LHR is nowadays a mature and very promising technology that is destined to replace current methods as the main optical tool for the targeted exploration of the chemical make-up of the atmosphere [6–12]. LHR instruments are robust, compact and cost-efficient, and feature an ultra-high sensitivity and an unmatched optical resolution. Besides this, and as demonstrated in this paper, a very simple modification of the traditional LHR spectral interrogation approach, such as that proposed by WM-LHR, provides outstanding improvements in many aspects of the LHR system operation that further qualify these systems as the atmospheric sounding tools of the future.

WM-LHR is based on a LHR system with a wavelength modulated LO laser that simplifies the optical architecture of the system by removing the optical chopper. On the TIR WM-LHR based on an EC-QCL presented in this paper, calibration-free WM-LHR has been demonstrated through a simple procedure that compensates intensity fluctuations from the RAM amplification level. This set-up, in comparison to a traditional LHR instrument, has demonstrated a superior SNR, a lessening in the requirements on the quality of the components and has opened the door for very wide range spectral characterization. These new features provide the potential to increase the accuracy and lower the cost of implementing a ground-based network of radiometers based on off-the-shelf components. Moreover, WM-LHR makes it feasible to tremendously multiply the spectral range of current systems by combining, when operated in conjunction with widely tunable monochromatic sources, a spectral range comparable to that of a FTS with ultra-high optical resolution and an enhanced

Optics EXPRESS

sensitivity. These characteristics promise to enable a new palette of applications that would range from atmospheric multiple analyte detection to deep space exploration.

Funding

Ministerio de Economía y Competitividad (TEC2017-86271-R); Österreichische Forschungsförderungsgesellschaft (861581 (ATMOSENSE)); Ministerio de Educación, Cultura y Deporte (Estancias de movilidad José Castillejo).

Acknowledgments

The work by P.M.-M. has been performed in the frame of the "Estancias de movilidad José Castillejo" from the Spanish Ministry of Education, Culture and Sports. P.M.-M. would also like to thank the Spanish Ministry of Economy and Competitiveness for supporting the project under the TEC2017-86271-R Grant. A.G., H. M. and B.L. acknowledge financial support received from the Austrian Research Promotion Agency FFG within the project 861581 (ATMOSENSE) of the ERA-NET Photonics program.

References

1. D. Wunch, G. C. Toon, J.-F. L. Blavier, R. A. Washenfelder, J. Notholt, B. J. Connor, D. W. T. Griffith, V. Sherlock, and P. O. Wennberg, "The total carbon column observing network," Philos Trans A Math Phys Eng Sci **369**(1943), 2087–2112 (2011).
2. F. Chevallier, N. M. Deutscher, T. J. Conway, P. Ciais, L. Ciattaglia, S. Dohe, M. Fröhlich, A. J. Gomez-Pelaez, D. Griffith, F. Hase, L. Haszpra, P. Krummel, E. Kyrö, C. Labuschagne, R. Langenfelds, T. Machida, F. Maignan, H. Matsueda, I. Morino, J. Notholt, M. Ramonet, Y. Sawa, M. Schmidt, V. Sherlock, P. Steele, K. Strong, R. Sussmann, P. Wennberg, S. Wofsy, D. Worthy, D. Wunch, and M. Zimnoch, "Global CO_2 fluxes inferred from surface air-sample measurements and from TCCON retrievals of the CO2 total column," Geophys. Res. Lett. **38**(24), L24810 (2011).
3. A. Kuze, H. Suto, M. Nakajima, and T. Hamazaki, "Thermal and near infrared sensor for carbon observation Fourier-transform spectrometer on the Greenhouse Gases Observing Satellite for greenhouse gases monitoring," Appl. Opt. **48**(35), 6716–6733 (2009).
4. C. Frankenberg, R. Pollock, R. A. M. Lee, R. Rosenberg, J.-F. Blavier, D. Crisp, C. W. O'Dell, G. B. Osterman, C. Roehl, P. O. Wennberg, and D. Wunch, "The Orbiting Carbon Observatory (OCO-2): spectrometer performance evaluation using pre-launch direct sun measurements," Atmos. Meas. Tech. **8**, 301–313 (2015).
5. D. R. Thompson, D. Chris Benner, L. R. Brown, D. Crisp, V. Malathy Devi, Y. Jiang, V. Natraj, F. Oyafuso, K. Sung, D. Wunch, R. Castaño, and C. E. Miller, "Atmospheric validation of high accuracy CO2 absorption coefficients for the OCO-2 mission," J. Quant. Spectrosc. Radiat. Transf. **113**(17), 2265–2276 (2012).
6. P. I. Palmer, E. L. Wilson, G. L. Villanueva, G. Liuzzi, L. Feng, A. J. DiGregorio, J. Mao, L. Ott, and B. Duncan, "Potential improvements in global carbon flux estimates from a network of laser heterodyne radiometer measurements of column carbon dioxide," Atmos. Meas. Tech. Discuss. (in review).
7. D. Weidmann, A. Hoffmann, N. Macleod, K. Middleton, J. Kurtz, S. Barraclough, and D. Griffin, "The methane isotopologues by solar occultation (MISO) nanosatellite mission: spectral channel optimization and early performance analysis," Remote Sens. **9**(10), 1073 (2017).
8. E. L. Wilson, A. J. DiGregorio, V. J. Riot, M. S. Ammons, W. W. Bruner, D. Carter, J. Mao, A. Ramanathan, S. E. Strahan, L. D. Oman, C. Hoffman, and R. M. Garner, "A 4 U laser heterodyne radiometer for methane (CH4) and carbon dioxide (CO_2) measurements from an occultation-viewing CubeSat," Meas. Sci. Technol. **28**(3), 035902 (2017).
9. A. Hoffmann, N. A. Macleod, M. Huebner, and D. Weidmann, "Thermal infrared laser heterodyne spectroradiometry for solar occultation atmospheric CO2 measurements," Atmos. Meas. Tech. **9**(12), 5975–5996 (2016).
10. E. L. Wilson, M. L. McLinden, J. H. Miller, G. R. Allan, L. E. Ott, H. R. Melroy, and G. B. Clarke, "Miniaturized laser heterodyne radiometer for measurements of CO2 in the atmospheric column," Appl. Phys. B **114**(3), 385–393 (2014).
11. T. Stangier, T. Hewagama, M. Sornig, G. Sonnabend, T. Kostiuk, M. Herrmann, and T. Livengood, "Thermal structure of Venus' nightside mesosphere as observed by infrared heterodyne spectroscopy at 10 μm," Planet. Space Sci. **113–114**, 359–368 (2015).
12. H. Nakagawa, S. Aoki, H. Sagawa, Y. Kasaba, I. Murata, G. Sonnabend, M. Sornig, S. Okano, J. R. Kuhn, J. M. Ritter, M. Kagitani, T. Sakanoi, M. Taguchi, and K. Takami, "IR heterodyne spectrometer MILAHI for continuous monitoring observatory of Martian and Venusian atmospheres at Mt. Haleakalā, Hawaii," Planet. Space Sci. **126**, 34–48 (2016).
13. H. R. Melroy, E. L. Wilson, G. B. Clarke, L. E. Ott, J. Mao, A. K. Ramanathan, and M. L. McLinden, "Autonomous field measurements of CO_2 in the atmospheric column with the miniaturized laser heterodyne radiometer (Mini-LHR)," Appl. Phys. B **120**(4), 609–615 (2015).

Optics EXPRESS

14. D. Weidmann and G. Wysocki, "High-resolution broadband (>100 cm^{-1}) infrared heterodyne spectro-radiometry using an external cavity quantum cascade laser," Opt. Express **17**(1), 248–259 (2009).
15. R. T. Menzies, "Remote detection of SO_2 and CO_2 with a heterodyne radiometer," Appl. Phys. Lett. **22**(11), 592–593 (1973).
16. R. T. Menzies and M. S. Shumate, "Air pollution: remote detection of several pollutant gases with a laser heterodyne radiometer," Science **184**(4136), 570–572 (1974).
17. P. Martín-Mateos, O. E. Bonilla-Manrique, and C. Gutiérrez-Escobero, "Wavelength modulation laser heterodyne radiometry," Opt. Lett. **43**(12), 3009–3012 (2018).
18. J. Hodgkinson and R. P. Tatam, "Optical gas sensing: a review," Meas. Sci. Technol. **24**(1), 012004 (2013).
19. A. Hoffmann, M. Huebner, N. Macleod, and D. Weidmann, "Spectrally resolved thermal emission of atmospheric gases measured by laser heterodyne spectrometry," Opt. Lett. **43**(16), 3810–3813 (2018).
20. G. B. Rieker, J. B. Jeffries, and R. K. Hanson, "Calibration-free wavelength-modulation spectroscopy for measurements of gas temperature and concentration in harsh environments," Appl. Opt. **48**(29), 5546–5560 (2009).